

# Collective Radiance and Dynamics in Multi-Level Atom Nano-Rings

Author: Guillem Lancis Beneyto

*Facultat de Física, Universitat de Barcelona, Diagonal 645, 08028 Barcelona, Spain.*

Advisor: Maria Moreno Cardoner

The collective spontaneous emission of an ensemble of atoms trapped in a ring configuration is studied when the interparticle distance is smaller than the transition wavelength. Here, interference effects between scattered fields can lead to the enhancement or suppression of the collective atomic decay rates from an excited state, a phenomenon known as superradiance or subradiance, respectively. In this work we study these phenomena in isotropic atoms with three possible degenerate transitions from the ground state to excited states, when a single excitation is present in the system. In addition, we study the excitation transport in the ring and show that subradiant states can be useful to enhance the efficiency in the process, compared to non-interacting atoms.

## I. INTRODUCTION

In quantum optics the ability to control atom-light interactions has been studied over decades for its relevance not only to fundamental physics, but also to many applications such as quantum metrology or quantum computation. Within all of these applications, spontaneous emission is a limitation because photons are emitted in random directions, representing a loss of information.

In diluted ultra-cold atomic ensembles, spontaneous emission of photons is typically assumed to occur at the same energy and rate as for an isolated atom. However, we study the case of dense atomic ensembles where atoms are separated by distances comparable to the atomic transition wavelength. In this case, the decay rate and frequency of the emitted photons is modified due to their coupling to the same electromagnetic field mode. This common coupling leads to dipole-dipole interactions through the exchange of virtual photons and collective spontaneous emission of photons, leading to the well-known phenomena of superradiance and subradiance.

When the emission of photons takes place at a rate much faster or slower than the single atom decay rate, the phenomenon of superradiance or subradiance, respectively, occurs. Dicke [1] already predicted this effect for molecules in a very small volume interacting with a homogeneous light field. Superradiant states have been experimentally detected with atoms [2, 4], trapped ions [3] and superconducting q-bits [6]. Moreover, despite subradiant states are more elusive due to their natural decoupling from radiative fields, they also have been recently detected in atomic ensembles [5]. Here, we focus on a different regime, where atoms are extended in real space and experience the field variations, interacting with the full set of three-dimensional optical modes. In this regime a strong dependence on the geometry is expected and we will focus on ring-shaped arrays.

Most previous works in this field focus on studying two-level atoms. Here, we extend these studies to multilevel atoms. In particular, we consider the  $J = 0 \rightarrow J = 1$  transition in isotropic atoms, where  $J$  is the electronic angular momentum. The three possible transitions from

$J = 0$  to a final state with  $m_J = -1$ ,  $m_J = 0$ ,  $m_J = 1$  (the so-called  $\sigma_-$ ,  $\pi$  and  $\sigma_+$  transitions, respectively) are degenerated in absence of any external field, and this richer internal structure may lead to new phenomena.

The work is organized as follows. First, we present the theoretical model used to describe atoms interacting with light, where multiple scattering and propagation of photons within the atomic media are taken into account to describe the dynamics of the system. Next, and to begin gaining some intuition, we study the emergence of collectively radiant states in the case of  $N$  two-level atoms in a ring-shaped array, with a single ground state and a single excited state. Then, we move to the case of multilevel atoms with  $J = 0 \rightarrow J = 1$  transition. Finally, we study the dynamics and excitation transport when the system is initialized with one atom of the array in the excited state. Throughout this work, we restrict to the case of a single collective excitation.

## II. THEORETICAL BACKGROUND

The system we study consists of  $N$  identical atoms trapped at fixed positions and forming a ring, with distance  $d$  between two consecutive atoms. We consider the  $J = 0 \rightarrow J = 1$  transition, where  $J$  is the electronic angular momentum, such that the atomic levels consist of a single ground state  $|g\rangle$  and three degenerated excited states  $|+1\rangle$ ,  $|0\rangle$  and  $|-1\rangle$ , with atomic transition energy  $\hbar\omega_0$ , as shown in Fig. 1.

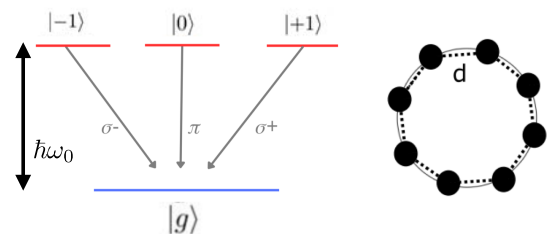


FIG. 1: Left: Level scheme of an atom with  $J = 0 \rightarrow J = 1$  transition. Applying an external magnetic field degeneration can be broken. Right: Sketch of a ring with  $N = 8$  atoms, being  $d$  the shortest distance between two consecutive atoms.

The atoms are in contact with a radiation field acting as a large reservoir with a short coherence time. One can integrate over the electromagnetic degrees of freedom and find the master equation governing the dynamics of the atomic degrees of freedom within the Born-Markov approximation [7]:

$$\dot{\rho} = -\frac{i}{\hbar} [H, \rho] + \mathcal{L}[\rho], \quad (1)$$

where  $\rho$  is the atomic density operator.  $\mathcal{L}$  is the Lindblad operator describing collective dissipation and defined as:

$$\mathcal{L}[\rho] = \sum_{\alpha, \beta} \sum_{i, j}^N \frac{\Gamma_{ij}^{\alpha\beta}}{2} \left( 2\sigma_j^{g\alpha} \rho \sigma_i^{\beta g} - \sigma_i^{\beta g} \sigma_j^{g\alpha} \rho - \rho \sigma_i^{\beta g} \sigma_j^{g\alpha} \right), \quad (2)$$

with  $\alpha, \beta = \{+1, 0, -1\}$ . Here  $\sigma_j^{g\alpha}$  and  $\sigma_j^{\alpha g}$  are the lowering and raising atomic operators respectively, that create or destroy a single excitation in the state  $|\alpha\rangle = | +1 \rangle, | 0 \rangle, | -1 \rangle$  of atom  $j$ . The Hamiltonian  $H$  describes the coherent exchange of excitations between the atoms, and can be written as:

$$H = \hbar \sum_{\alpha, \beta} \sum_{i, j=1}^N J_{ij}^{\alpha\beta} \sigma_i^{\alpha\beta} \sigma_j^{g\alpha}, \quad (3)$$

with  $\alpha, \beta = \{+1, 0, -1\}$ . The couplings are defined as  $J_{ij}^{\alpha\beta} = \text{Re}[\mathcal{G}_{ij}^{\alpha\beta}]$  and  $\Gamma_{ij}^{\alpha\beta} = -2\text{Im}[\mathcal{G}_{ij}^{\alpha\beta}]$ , being  $\mathcal{G}_{ij}^{\alpha\beta} = (3\pi\Gamma_0/k_0) \hat{\phi}_i^\alpha \cdot \overleftrightarrow{G}(\mathbf{r}_i - \mathbf{r}_j, \omega_0) \cdot \hat{\phi}_j^\beta$ . Here  $k_0 = \omega_0/c$ ,  $\Gamma_0 = \omega_0^3 \varphi^2 / 3\pi\epsilon_0 \hbar c^3$  is the spontaneous emission rate of an isolated atom,  $\varphi$  is the dipole moment strength,  $\hat{\phi}_i^\alpha$  is the dipole moment orientation associated with transition to state  $|\alpha\rangle$ , and  $\overleftrightarrow{G}(\mathbf{r}_i - \mathbf{r}_j, \omega_0)$  is the Green's tensor describing the electromagnetic field propagation between two atoms located at  $\mathbf{r}_i$  and  $\mathbf{r}_j$ :

$$\overleftrightarrow{G}(\mathbf{r}, \omega_0) = \frac{e^{ik_0 r}}{4\pi k_0^2 r^3} \left[ (k_0^2 r^2 + ik_0 r - 1) \mathbb{1} + (-k_0^2 r^2 - 3ik_0 r + 3) \frac{\mathbf{r} \otimes \mathbf{r}}{r^2} \right]. \quad (4)$$

In this work, we restrict to at most one atomic excitation in the system. In this case, the first term in the Lindblad operator (also called recycling term) only modifies the ground state population. The dynamics in the excitation sector are then governed by:

$$\dot{\rho}_{ee} = -\frac{i}{\hbar} \left( H_{\text{eff}} \rho_{ee} - \rho_{ee} H_{\text{eff}}^\dagger \right), \quad (5)$$

where  $\rho_{ee}$  denotes the sub-block of the density matrix only involving single excitation states. Here  $H_{\text{eff}}$  is a non-Hermitian Hamiltonian of the form:

$$H_{\text{eff}} = \hbar \sum_{\alpha, \beta} \sum_{i, j=1}^N \left( J_{ij}^{\alpha\beta} - i \frac{\Gamma_{ij}^{\alpha\beta}}{2} \right) \sigma_i^{\alpha g} \sigma_j^{g\beta}, \quad (6)$$

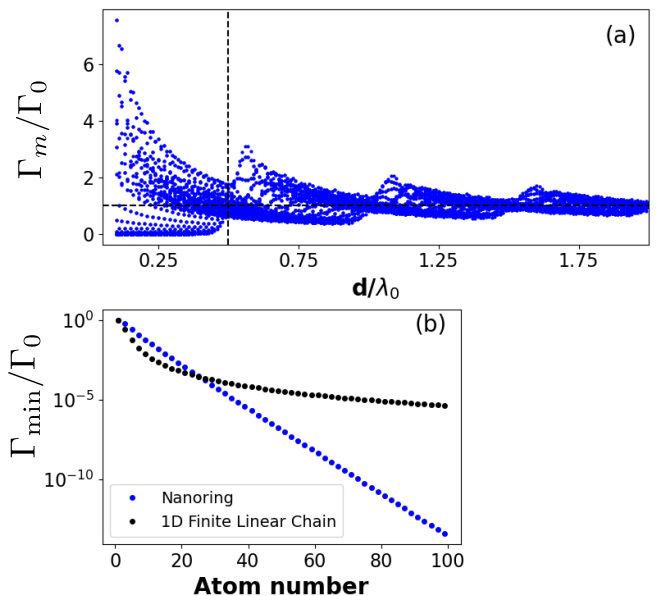


FIG. 2: (a) Collective decay rates (in units of single atom decay rate  $\Gamma_0$ ) as a function of  $d/\lambda_0$ , for a ring with  $N = 50$  atoms. We observe the emergence of many subradiant modes for  $d/\lambda_0 \lesssim 1/2$ . (b) Comparison between the minimum decay rate (in units of  $\Gamma_0$ ) for a ring (blue) and a linear (black) chain, as a function of atom number  $N$  and  $d/\lambda_0 = 0.3$ .

with  $\alpha, \beta = \{+1, 0, -1\}$ . We also redefine the self-interaction term  $J_{ii}^{\alpha\beta} = 0$ , to avoid a divergence that can be renormalized, and only represents a global frequency shift. Despite being a non-Hermitian matrix, we can still diagonalize  $H_{\text{eff}}$  and find a set of eigenvalues  $\{\lambda_m\}$  and eigenstates, that can be interpreted as collective modes involving all lattice sites. The imaginary and real parts of the eigenvalues are related to the collective spontaneous emission rate  $\Gamma_m$  and frequency shifts  $J_m$  of the modes, respectively:  $\Gamma_m = -2\text{Im}(\lambda_m)$ , and  $J_m = \text{Re}(\lambda_m)$ .

### III. RESULTS

#### A. Collective radiance in two-level atom nanorings

We first study how the spontaneous emission rate of an atom is modified in presence of other atoms. For pedagogical reasons, we start by studying the collective decay rates  $\Gamma_m$  of atoms with only one possible transition (*i.e.*, two-level). We choose the ring configuration (see Fig. 1) with atoms transversally polarized to the plane containing the ring (that is, only consider the  $\pi$  transition), and restrict to the single excitation manifold as mentioned.

We exactly diagonalize the effective Hamiltonian Eq.(6) for this atomic configuration in the single-excitation subspace (note that  $H_{\text{eff}}$  conserves the total number of excitations), and find the eigenmodes and corresponding eigenvalues, for different values of  $d$ . The result for the collective decay rates versus the distance  $d$

is shown in Fig. 2(a). We observe that strongly modified decay rates compared to the single atom one ( $\Gamma_0$ ) emerge, as expected, when  $d/\lambda_0 \rightarrow 0$ . In contrast, for  $d/\lambda_0 > 1$  we obtain  $\Gamma \rightarrow \Gamma_0$ , as for isolated atoms.

The emergence of perfectly dark modes is well understood in an infinite linear chain [8]. This gives an intuitive explanation of the result in the very large ring limit ( $R/\lambda_0 \gg 1$ ), where the curvature is small. Due to the discrete translational invariance of the infinite chain, eigenmodes follow Bloch's theorem. Then, single excitation eigenstates are plane-waves of the form  $|q_x\rangle = \sum_j e^{iq_x \cdot x_j} |j\rangle / \sqrt{N}$ , where  $|j\rangle = \sigma_j^{eg} |g\rangle$  corresponds to an excitation at site  $j$ , and  $q_x$  is the quasi-momentum defined within the first Brillouin zone ( $|q_x| \leq \frac{\pi}{d}$ ). It can be shown [8] that the electromagnetic field generated by such state is a superposition of plane-waves with momentum  $\mathbf{k}$ , obeying  $|\mathbf{k}| = \frac{2\pi}{\lambda_0} = k_0$  due to Maxwell's equations, and with parallel component to the chain  $k_x = q_x + Q$ , where  $Q$  is any vector from the reciprocal lattice. Thus, for  $q_x$  outside the light-line ( $|q_x| \geq \frac{2\pi}{\lambda_0}$ ), the perpendicular momentum components of the field are imaginary and the field is evanescent outside the structure. This leads to guided optical modes through the atomic chain with perfect inability to radiate energy to the environment. Taking into account the Brillouin zone boundary leads to the condition  $d \leq \lambda_0/2$  for the existence of dark modes. In Fig. 2(a), this behavior is approximately found, as we observe the emergence of many dark modes for  $d/\lambda_0 \lesssim 1/2$ . In contrast to the linear infinite chain, the modes are not perfectly dark, as they weakly radiate over the finite radius of curvature.

Furthermore, we can compare for fixed  $d/\lambda_0 = 0.3$ , the minimum decay rate obtained for the geometry of the ring, and for a linear chain, both with transverse polarization. As shown in Fig. 2(b) the minimum decay rate of the finite linear chain has a polynomial scaling with the number of atoms  $N$ , while in the nano-ring structure it shows an exponential dependence. For  $N \gtrsim 25$  darker modes appear in the ring-shaped structure for the chosen  $d/\lambda_0$ . This can be understood in the following way: for the finite linear chain the fields scatter from the boundaries while in the nano-ring configuration, with periodic boundary conditions, there is a higher suppression of these modes due to the closed configuration.

## B. Collective radiance in multilevel atom nanorings

We now generalise the above discussion to atoms with more than one excited state, in particular, we consider the  $J = 0 \rightarrow J = 1$  transition described before. In the following, we propose a semi-analytical solution for the single-excitation eigenmodes. In this case, the effective Hamiltonian Eq.(6) projected onto the single excitation manifold is a  $3N \times 3N$  matrix, and it can be written:

$$H_{1\text{exc}} = \sum_{\alpha, \beta} \sum_{i, j=1}^N H_{i, j}^{\alpha, \beta} |j, \alpha\rangle \langle i, \beta|, \quad (7)$$

where  $\alpha, \beta = \{-1, 0, +1\}$  label the three different excited states. Here  $|j, \alpha\rangle$  represents a state where all atoms are in the ground state except atom  $j$ , which is in the  $\alpha$  excited state.

Taking into account the discrete rotational symmetry of the ring, we now propose a change to the basis with well defined angular momentum:

$$|m, \alpha\rangle = \frac{1}{\sqrt{N}} \sum_j e^{i2\pi m j/N} |j, \alpha\rangle \quad (8)$$

where  $m \in \{0, \pm 1, \pm 2, \dots, \pm[(N-1)/2]\}$ . In order to preserve full rotational symmetry, and using the fact that the excited states are degenerate, we will also change the initial atomic dipole transition basis  $\{\sigma^+, \sigma^-, \pi\}$  into a polar basis, where dipoles are oriented along the radial ( $\hat{r}$ ), tangential ( $\hat{\phi}$ ) and  $\hat{z}$ -direction. One can show that working in this basis we arrive at a simplified form of the Hamiltonian:

$$H_{1\text{exc}} = \sum_{\alpha, \beta} \sum_m H_m^{\alpha, \beta} |m, \alpha\rangle \langle m, \beta|, \quad (9)$$

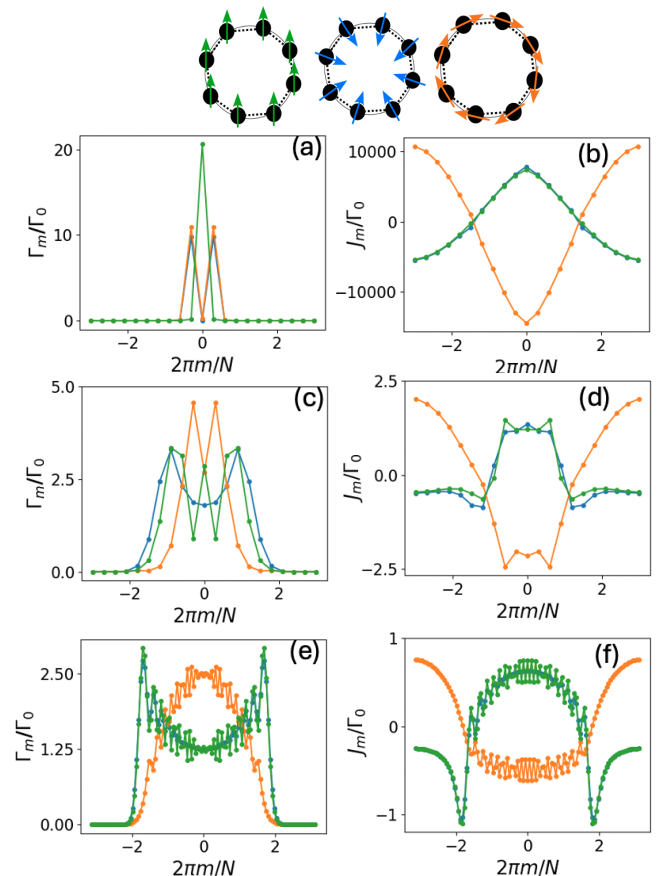


FIG. 3: Collective decay rates (left) and frequency shifts (right), in units of single atom decay rate  $\Gamma_0$ . (a) and (b):  $d/\lambda_0 = 0.01, N = 21$  (Dicke limit); (c) and (d):  $d/\lambda_0 = 0.2, N = 21$  ( $R \sim \lambda_0$ ); (e) and (f):  $d/\lambda_0 = 0.3, N = 111$  (quasi-linear chain). Different bands have predominantly the dipole orientation shown in the inset with the same color code.

with  $H_m^{\alpha\beta} = \sum_{j=1}^N G^{\alpha\beta}(\mathbf{r}_j) \exp(i2\pi mj/N)$ , where  $\mathbf{r}_j$  runs over all possible vectors connecting a given site and any site of the ring, including itself. For every value of  $m$  we then get a  $3 \times 3$  matrix that can be exactly diagonalized to find the eigenvalues  $\lambda_{m,\eta}$  ( $\eta = 1, 2, 3$ ), from which we obtain the collective frequency shifts  $J_{m,\eta} = \text{Re}(\lambda_{m,\eta})$  and decay rates  $\Gamma_{m,\eta} = -2\text{Im}(\lambda_{m,\eta})$ . The three possible values of  $\eta$  for each  $m$  gives rise to a band structure with three different bands.

The results for three different cases (changing  $d/\lambda_0$  and  $N$ ) are shown in Fig. 3. Moreover, we find that the corresponding eigenmodes of the three bands have components predominantly in  $\hat{r}$ ,  $\hat{\varphi}$  or  $\hat{z}$  directions (result not shown here). The color code used to plot the different eigenvalues is the same used in the sketch of the dipole orientations in the same figure (blue, orange and green for radial, tangential and z-polarization, respectively).

Panels (a) and (b) in Fig. 3 are for  $d/\lambda_0 = 0.01$  and  $N = 21$  which is in the so-called Dicke regime, corresponding to the particles very close to each other experiencing an almost homogeneous field. In the case of the dipoles oriented along  $\hat{z}$  there is a perfect radiant state for  $m = 0$  with decay rate  $N\Gamma_0$ , while all other are completely dark. Intuitively, in the  $m = 0$  case all dipoles are parallel and radiating in phase, thus the field is amplified. In contrast, in the case of dipoles oriented along the radial or tangential direction there is a subradiant state at  $m = 0$  due to the suppression of dipole moments by pairs when atoms are so close. The radiant states at  $m = \pm 1$  with decay rate  $\frac{N}{2}\Gamma_0$  can be explained as the phase of dipole  $j$  given by  $e^{i\frac{2\pi mj}{N}}$  rotates the dipole to align it parallel to the others.

Panels (e) and (f) are for  $d/\lambda_0 = 0.3$  and  $N = 111$  atoms, corresponding to the limit where the nano-ring resembles locally to an infinite linear chain. Dipoles oriented along  $\hat{z}$  or  $\hat{r}$  tend to the transverse polarization case for the linear chain, so the two bands tend to overlap. Instead, the dipoles oriented along  $\hat{\varphi}$  are in a head-to-tail configuration, resembling the parallel polarization case of the linear chain. The collective shifts show a completely different behavior in both cases, inverting its sign.

Finally, an intermediate case with  $d/\lambda_0 = 0.2$  and  $N = 21$  is shown in panels (c) and (d), where the bands start to be similar to the infinite chain limit but still preserve some properties of the Dicke Limit.

### C. Single Excitation Transport in Nano-Rings of Multilevel Atoms

As discussed before, the dynamics in the single excitation sector are governed by Eq.(5). This allows to work in a wave-function representation, whose norm is not conserved due to the non-Hermitian character of  $H_{\text{eff}}$ .

We will consider an initial state that is prepared with a single excitation at site  $j = 0$  and polarized along the  $\hat{x}$  axis (also coinciding with the radial direction), that is,  $|\Psi(0)\rangle = (|j, +1\rangle + |j, -1\rangle)/\sqrt{2}$ . This initial state can also be written as a superposition of the eigen-

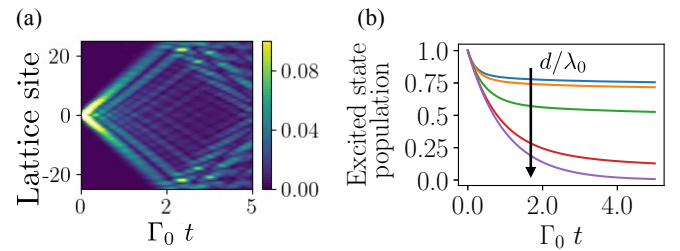


FIG. 4: (a) Local excited state population  $p_j(t) = 2p_{j,\pm 1}(t)$  versus time for an initially localized excitation with dipole moment oriented along the radial direction. ( $d/\lambda_0 = 0.08$ ). (b) Total Excited state population versus time for  $d/\lambda_0 = 0.08, 0.1, 0.2, 0.4, 1$ . ( $N = 51$ )

modes with well defined angular momentum  $|\Psi(0)\rangle = (1/\sqrt{N}) \sum_{\eta} \sum_m c_m^{\eta}(0) |m, \eta\rangle$ , where  $c_m^{\eta}(0)$  are complex coefficients. From Eq.(5) the time-evolved state takes the form:

$$|\Psi(t)\rangle = \frac{1}{\sqrt{N}} \sum_{\eta} \sum_m c_m^{\eta}(0) e^{-iJ_{m,\eta}t} e^{-\Gamma_{m,\eta}t/2} |m, \eta\rangle, \quad (10)$$

with  $\eta = 1, 2, 3$ . In this equation it is important to note the role of every term appearing in the time-evolution:  $e^{-iJ_m t}$  introduces a different phase to every eigenmode without changing the modulus, while  $e^{-\Gamma_m/2 t}$  represents the collective character of the dissipation decreasing the mode occupation (and the norm of the state).

We now compute the time evolution from Eq.(10) and the occupation of the locally excited states, that is,  $p_{j,\pm 1}(t) = |\langle j, \pm 1 | \Psi(t) \rangle|^2$  ( $j = 1, \dots, N$ ). Due to the symmetry in the initial state, we have that  $p_{j,+1}(t) = p_{j,-1}(t) = p_j(t)/2$ , and also, because of the system geometry, the state  $|0\rangle$  is decoupled and remains not occupied over time. In Fig. 4(a) we can see how the excitation initially localized at site  $j = 0$  with  $\hat{x}$  polarization evolves over time and rapidly becomes completely delocalised along the lattice. The dephasing between the different modes, also gives rise to interference fringes. In Fig. 4(b) we plot the total excited state population  $p(t) = \sum_{j=1}^N p_j(t)$  versus time, for different values of  $d/\lambda_0$ , and we observe how it decays rapidly until saturating at a fixed value that decreases with  $d/\lambda_0$ . This is because superradiant states decay very fast, while subradiant modes (which do not radiate the excitation away) remain populated. Increasing  $d/\lambda_0$  reduces the number of subradiant states and hence the probability of the excitation survival, as expected.

The previous discussion becomes clearer when plotting the occupation of the modes with well defined angular momentum  $m$ , as shown in Fig. 5(a) and (b), where we choose a polar basis for the polarization degree of freedom. Superradiant states are those with low  $|m|$  at the center of the Brillouin zone, which quickly become unoccupied, as these are the states whose population does not survive over time. In contrast, the population of subradi-

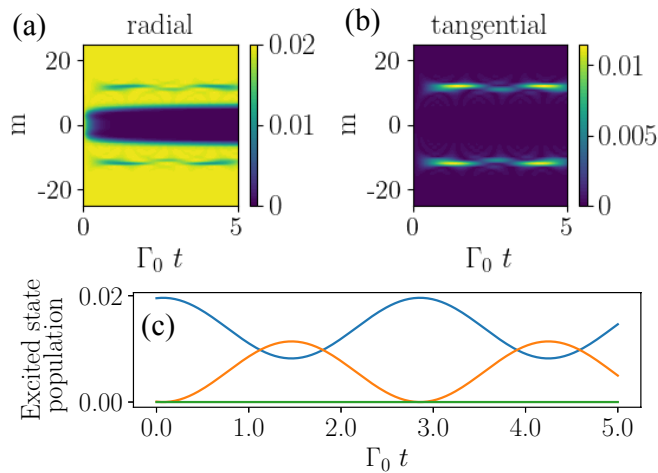


FIG. 5: (a) Excited state population of each collective mode with well defined angular momentum  $m$  for the radial (a) and tangential (b) components, versus time. The occupation of radiant modes quickly decays, while it survives in the sub-radiant modes. (c) The same for  $m = \lfloor N/4 \rfloor$  (corresponding approximately to the crossing point of the two energy bands). We observe oscillations between the radial (blue) and tangential (orange) components. ( $N = 51$ ,  $d/\lambda_0 = 0.08$ ).

ant states (higher value of  $|m|$ ) survive longer in the ring. Moreover we can see how starting with an excited state localized in the lattice (which is a superposition of all angular momentum states) and with  $\hat{r}$  polarization does not mix to the  $\hat{\varphi}$  polarization except for some values of  $m$ . These are the values of  $m$  in Fig. 3 where frequency shift bands intersect ( $|m| \sim N/4$ ). For these values the excitation population oscillates between between the  $\hat{r}$  and  $\hat{\varphi}$  transitions, as shown in Fig. 5(c), as the eigenmodes are in a superposition of both components.

#### IV. CONCLUSIONS

The collective radiative properties of a ring-shaped array of  $N$  atoms is studied. Coupling to the same radia-

tion mode leads to strongly modified decay rates and frequency shifts when the interparticle distance is  $d/\lambda_0 \lesssim 1$ , leading to superradiance and subradiance phenomena. We start by studying the case of two-level atoms in the single excitation manifold, for which extremely dark modes emerge when  $d/\lambda_0 \lesssim 1/2$ . Then, we extend this analysis to multilevel atoms with  $J = 0 \rightarrow J = 1$  transition. In this case the eigenmodes still have well defined angular momentum and display a structure with three bands associated with the internal degrees of freedom.

Next, we study the dynamics of an initially excited state localized at a given site. We observe that thanks to the subradiant states the survival probability of the excited population can be very large compared to isolated atoms. Moreover, due to the band structure of the eigenmodes and the degeneracy at  $|m| \sim N/4$  we observe oscillations between the population of the excited states in the radial and tangential components.

In order to continue with this work, it would be interesting to consider the transport of an initial wavepacket, where the excitation is delocalized over several sites. Preparing the wavepacket centered around a subradiant state for which the dispersion is approximately linear, one can in principle achieve a longer lifetime transport of the wavepacket preserving its shape. Also controlling dynamics using an external magnetic field that breaks the degeneracy between the three possible atomic transitions could be used for storage and transport control. The effect of atomic disorder in the dynamics can also be studied. Finally, it would be interesting to explore the eigenmode structure in higher excitation manifolds.

#### Acknowledgments

I would like than my advisor, Dra. Maria Moreno not only for introducing me such an outstanding field of research, but also for her mentorship and kindness. Also to my parents and sister for their unconditional support.

- 
- [1] R. H Dicke , *Coherence in spontaneous radiation processes*, Phys. Rev. **93**, 99-110 (1954).  
[2] M. Gross, C. Fabre, P. Pillet and S. Haroche , *Observation of near-infrared Dicke superradiance on cascading transitions in atomic sodium*, Phys. Rev. **36**, 1035 (1976).  
[3] R. G. DeVoe and R. G. Brewer, *Observation of superradiant and subradiant spontaneous emission of two trapped ions*, Phys. Rev. Lett. **76**, 2049 (1996).  
[4] J. A. Mlynek, *et al.*, *Observation of Dicke superradiance for two artificial atoms in a cavity with high decay rate*, Nat. Comm. **5**, 5186 (2014).  
[5] W. Guerin, *et al.*, *Subradiance in a large cloud of cold atoms*, Phys. Rev. Lett. **116**, 083601 (2016).  
[6] P. Solano, P. Barberis-Blostein, F. K. Fatemi, L. A. Orozco and S. L. Rolston, *Super-radiance reveals infinite-range dipole interactions through a nanofiber*, Nat. Comm. **8**, 1857 (2017).  
[7] Daniel A. Steck, *Quantum and Atom Optics*, available online at: <https://steck.us/teaching>, 144-146 (2023).  
[8] A. Asenjo-Garcia, M. Moreno-Cardoner, A. Albrecht, H.J. Kimbre and D.E. Chang, *Exponential improvement in photon storage fidelities using subradiance and "selective radiation" in atomic arrays*, Phy. Rev. X **7**, 031024 (2017).  
[9] J. A Needham, I. Lesanovsky and B. Olmos *Subradiance-protected excitation transport*, New J. Phys. **21**, 073061 (2019).